Geophysical Journal International

Geophys. J. Int. (2020) **222,** 1898–1908
Advance Access publication 2020 June 10
GJI Gravity, Geodesy and Tides

doi: 10.1093/gji/ggaa240

Speed and accuracy improvements in standard algorithm for prismatic gravitational field

Toshio Fukushima

National Astronomical Observatory / SOKENDAI, Ohsawa, Mitaka, Tokyo 181-8588*, Japan. E-mail: ToShio.FukuShima@nao.ac.jp*

Accepted 2020 May 11. Received 2020 May 7; in original form 2019 August 23

SUMMARY

By utilizing the addition theorems of the arctangent function and the logarithm, we developed a new expression of Bessel's exact formula to compute the prismatic gravitational field using the triple difference of certain analytic functions. The use of the new expression is fast since the number of transcendental functions required is significantly reduced. The numerical experiments show that, in computing the gravitational potential, the gravity vector, and the gravity gradient tensor of a uniform rectangular parallelepiped, the new method runs 2.3, 2.3 and 3.7 times faster than Bessel's method, respectively. Also, the new method achieves a slight increase in the computing precision. Therefore, the new method can be used in place of Bessel's method in any situation. The same approach is applicable to the geomagnetic field computation.

Key words: Geopotential theory; Gravity anomalies and Earth structure; Magnetic anomalies: modelling and interpretation.

1 INTRODUCTION

Remarkable is the development of various studies of topographic gravitational and/or geomagnetic field (Tsoulis 2001; Featherstone & Kirby 2002; Hirt *et al.* 2016, 2019; Ren *et al.* 2017; Yamazaki *et al.* 2017; Hirt 2018). This achievement has been encouraged by the recent progress in the production of detailed digital elevation model (DEM, Smith & Sandwell 2003; Rodriguez *et al.* 2006; Amante 2009; Tachikawa *et al.* 2011). Among them, the Geospatial Information Authority of Japan has issued a DEM covering the whole land area of Japan with a very fine spatial resolution on the ground surface as small as 0.2 arcsec (Geospatial Information Authority of Japan 2012), which corresponds to 5.0 and 6.2 m in the east–west and north–south directions, respectively. Refer to Fig. 1 of our previous work (Fukushima 2020) showing the 2-D feature of a slope near Mt Fuji.

In treating the surface profiles with such ragged feature in the computation of the topographic field of gravity and/or geomagnetism, commonly used is the decomposition of the surface land mass into an assembly of rectangular parallelepiped, or the so-called prisms (Bessel 1813; Mollweide 1813; Kellogg 1929; MacMillan 1930; Mader 1951; Nagy 1966, 1988; Banerjee & Das Gupta 1977; Rao & Babu 1991, 1993; Garcia-Abdeslem 1992; Nagy *et al.* 2000; Garcia-Abdeslem 2005; Heck & Seitz 2007; Wild-Pfeiffer 2008; Zhang & Jiang 2017; Jiang *et al.* 2017, 2018; Fukushima 2018, 2020). Indeed, a prism serves as an essential building block in geodesy, geophysics and planetary sciences (Heiskanen & Moritz 1967; Moritz 1980; Forsberg & Tscherning 1981; Blakeley 1996; Jekeli 2007; Stacey & Davis 2008; de Pater & Lissauer 2010).

However, it is also true that the computational burden to evaluate its gravitational field is fairly large even if the density profile of the prism is as simple as constant. For example, once Forsberg emphasized in his treatise (Forsberg 1984, p. 28) as follows:

> ... evaluation of the complex exact prism formulas would often become prohibitive in terms of computer time...

This is partly because the number of prisms to be computed are too many in the practical applications. In order to circumvent this problem, three approaches have been proposed: (i) the reduction of the number of prisms based on the accuracy estimates of the input data (Kalmár *et al.* 1995; Benedek *et al.* 2018), (ii) the utilization of parallel computing (Hirt *et al.* 2016, 2019) and (iii) the conditional switch to an approximate formula using the truncated Taylor series expansion (Fukushima 2020).

Nevertheless, there remains an essential issue: the computation of the prismatic gravitational formulae is time-consuming itself, namely even if the number of prisms is only one. This is clearly demonstrated in Table 1 listing the averaged CPU times measured at a modern PC to compute various combinations of the gravitational potential, the three components of the gravitational acceleration vector, and the six independent components of the gravity gradient tensor of a single uniform prism. A reason exists for this heavy computational burden. As summarized by Nagy *et al.* (2000), Bessel's method (Bessel 1813) to evaluate the exact formulae demands the direct evaluation of certain

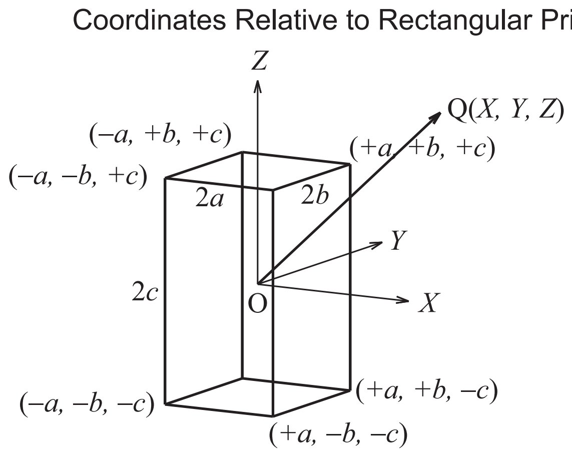

Figure 1. Coordinates relative to rectangular prism. Depicted is a diagram showing the coordinates (X, Y, Z) of an arbitrary point Q referred to O, the geometric centre of a rectangular prism of the size $2a \times 2b \times 2c$. Additionally shown are the coordinates of several vertices of the prism.

analytic functions, termed the potential functions, at 8 vertices of the given prism. Refer to Table 2 showing the number of computational operations required in the evaluation of the exact analytical formulae of various combinations of the gravitational field components of a uniform rectangular prism (Nagy *et al.* 2000).

Apart from the square root and four arithmetic operations, the potential functions contain two transcendental functions; the arctangent function and the logarithm (Bessel 1813). Even by using the latest CPUs, the computational time of these transcendental functions is fairly large when compared to those of the multiplications and addition/subtractions, say 30–160 times more as shown in Table 3.

Therefore, from a practical viewpoint, it is crucial to reduce the number of these transcendental functions in the evaluation of the exact formulae without any degrade in the computational precision. Indeed, the usage of the logarithm can be reduced by appropriately utilizing its subtraction theorem (Olver *et al.* 2010, formula 4.8.1):

$$\log X - \log Y = \log\left(\frac{X}{Y}\right). \tag{1}$$

This logarithmic compaction is classic. Indeed, it was adopted by Mollweide (1813) in expressing his analytic formula of the gravity vector. Refer to the usage in the potential computation (MacMillan 1930, pp.78 and 79) where not 24 but 12 logarithms appear. Also, the arctangent function is known to have a subtraction theorem (Bronshtein & Semendyayev 2015, formula 2.160) as

$$\tan^{-1} X - \tan^{-1} Y = \tan^{-1}\left(\frac{X-Y}{1+XY}\right) + \begin{cases} 0, & (XY > -1), \\ +\pi, & (XY < -1,\ X > 0), \\ -\pi, & (XY < -1,\ X < 0), \end{cases} \tag{2}$$

which is not strictly general, and therefore must be augmented for the special case, $XY = -1$, as

$$\tan^{-1} X - \tan^{-1} Y = \begin{cases} +\pi/2, & (XY = -1,\ X > 0), \\ -\pi/2, & (XY = -1,\ X < 0). \end{cases} \tag{3}$$

These correct expressions of the subtraction theorem of the arctangent function are not so popular in the existing literature and the standard textbooks on calculus and numerical analysis (Faires & Faires 1989; Henry & Penny 2002; Stewart 2014), where the existence of the ambiguous factors, $\pm\pi$ or $\pm\pi/2$, is ignored.

Note that the usage of the two-argument arctangent function, $atan2(y, x)$, is not generally able to resolve this ambiguity, say by rewriting the theorem as

$$\tan^{-1} X - \tan^{-1} Y = atan2\,(X - Y, 1 + XY)\,. \tag{4}$$

This is because $atan2(y, x)$ has been introduced by many different computer scientists, and thus, its function value range does depend on the computer language. Indeed, the range is defined as $[-\pi, \pi]$ in C and C++ but as $(-\pi, \pi]$ in Fortran. As a result, the Fortran implementation cannot cover the case, $\tan^{-1}X - \tan^{-1}Y = -\pi$.

At any rate, it is natural to anticipate that an adequate usage of these theorems will save the CPU time of the evaluation without loss of accuracy. In fact, there exist many works utilizing these theorems (Strakhov *et al.* 1986; Strakhov & Lapina 1986; Pohanka 1988; Ivan 1990; Pohanka 1990; Rao & Babu 1991, 1993; Holstein & Ketterridge 1996; Pohanka 1998; Holstein *et al.* 1999). In this short paper, we developed a new procedure to evaluate the triple difference formulae (Bessel 1813; Nagy *et al.* 2000) quickly by appropriately using the addition theorems. Consequently, the number of transcendental functions is reduced as shown in Table 2, and therefore an acceleration of the gravitational field computation is realized as already listed in Table 1. Below, we describe the new method in Section 2, and illustrate the results of its numerical experiments in Section 3.

Table 1. Computational cost of prismatic gravitational field. Listed are the averaged value of the CPU time to compute various combinations of the gravitational field components, namely (i) the gravitational potential, V, (ii) the jth rectangular component of the gravity vector, g_j and (iii) the jkth rectangular component of the gravity gradient tensor, Γ_{jk}, of a uniform rectangular prism. Compared are Bessel's method (Bessel 1813; Nagy *et al.* 2000) and the new method. The unit of CPU times is nanosecond at a consumer PC with the Intel Core i7-8750H CPU running at 2.20 GHz clock.

Combination	Bessel (unit:ns)	New (unit:ns)
V	557	242
Any of g_j	311	111
All g_j	576	250
Any of Γ_{jj}	124	39
Any of Γ_{jk} ($j \neq k$)	150	36
All Γ_{jk}	580	157
V and all of g_j	597	254
V, all g_j, and all Γ_{jk}	624	264

Table 2. Number of operations to compute the gravitational field of a uniform rectangular prism. Compared are the number of integer and floating point operations required in Bessel's method (Bessel 1813; Nagy *et al.* 2000) and the new method to compute the exact analytic formulae of various combinations of the gravitational field components, namely (i) the gravitational potential, V, (ii) the jth rectangular component of the gravity vector, g_j and/or (iii) the jkth rectangular component of the gravity gradient tensor, Γ_{jk}. Note that the number of arithmetic operations depends on the numerical value of input arguments in order to avoid the loss of information in the computation of logarithmic terms like $\ln(R+X)$ when $X < 0$. Meanwhile, the integer arithmetic are only used in the new method.

	Bessel						New						
	Floating point						Integer	Floating point					
Combination	+, −	∗	/	sqrt	atan	log	+, −	+, −	∗	/	sqrt	atan	log
V	127–158	24–96	24–48	8	24	24	12	127	175–187	18	8	6	12
Any of g_j	55–87	72–120	8–24	8	8	16	4	55	70–74	14	8	2	4
All g_j	95–143	168–240	24–48	8	24	24	12	125	174–186	18	8	6	12
Any of Γ_{jj}	23	48	8	8	8	0	6	25	59	1	8	1	0
Any of Γ_{jk} ($j \neq k$)	31–47	24–48	0–8	8	0	8	0	22	8–9	1	8	0	1
All Γ_{jk}	47–95	96–168	0	8	24	24	18	75	180–183	6	8	3	3
V and all g_j	161–212	248–320	24–48	8	24	24	12	154	193–205	18	8	6	12
V, all g_j, and all Γ_{jk}	203–254	248–320	24–48	8	24	24	12	160	193–205	18	8	6	12

2 FAST COMPUTATION OF ANALYTICAL FORMULAE OF GRAVITATIONAL FIELD GENERATED BY HOMOGENEOUS RECTANGULAR PRISM

2.1 Bessel's method

First of all, let us review the method developed by Bessel (1813) and summarized in Nagy *et al.* (2000) to compute (i) the gravitational potential, V, (ii) the jth rectangular component of the gravity vector, g_j and (iii) the jkth rectangular component of the gravity gradient tensor, Γ_{jk}, of a uniform rectangular prism where j and k are the coordinate indices, X, Y or Z. Assume that (i) the prism is of the size, $2a \times 2b \times 2c$, (ii) its geometric centre O is located at the coordinate origin and (iii) the coordinates of an arbitrary evaluation point Q are designated as (X, Y, Z), as seen in Fig. 1. Thus, the coordinates of the eight vertices of the prism become ($\pm a$, $\pm b$, $\pm c$).

For conciseness, we introduce the coordinates of the evaluation point relative to the vertices as

$$X_P \equiv X - a, \quad X_M \equiv X + a, \quad Y_P \equiv Y - b, \quad Y_M \equiv Y + b, \quad Z_P \equiv Z - c, \quad Z_M \equiv Z + c, \tag{5}$$

satisfying the conditions

$$X_P < X_M, \quad Y_P < Y_M, \quad Z_P < Z_M. \tag{6}$$

Then, we compute V, g_j and Γ_{jk} of the prism acting on the point, (X, Y, Z), by the evaluation of the triple differences of certain analytic functions, U, U_j and U_{jk}, which we name the potential functions, as

$$V = G\rho\Delta_3 U, \quad g_j = G\rho\Delta_3 U_j, \quad \Gamma_{jk} = G\rho\Delta_3 U_{jk}, \tag{7}$$

where (i) G is Newton's constant of universal attraction, (ii) ρ is the constant mass density of the prism and (iii) Δ_3 is the triple difference operator defined for an arbitrary three-variable function, $f(X, Y, Z)$, as

$$\Delta_3 f \equiv f_{PPP} - f_{PPM} - f_{PMP} - f_{MPP} + f_{PMM} + f_{MPM} + f_{MMP} - f_{MMM}. \tag{8}$$

Table 3. Instruction table of the latest Intel Core CPU. Shown are the number of instructions, N, and the latency, L, of some basic integer and floating point operations and mathematical functions at the Intel CPU/FPUs with the code name Skylake (Vog 2019, p. 238). They are listed in the increasing order of L. Note that these results are the same for the Coffeelake CPU/FPUs including the Intel Core i7-8750H used in the numerical experiments. In the table, (i) N denotes the number of cycles required by the micro operations in the fused mode, which is roughly called 'throughput', while (ii) L is the number of cycles needed until the total operations are completed at the FPU and returned to the CPU, which is usually named 'latency'. In general, the actual CPU times are between these two numbers depending on the compiled microcodes using various optimization options. The latency L is not constant for the division and the square root operations since they are executed by the Newton method, and therefore the number of its iteration depends on the numerical value of input arguments. In the case of mathematical functions, N and/or L vary because, depending on the numerical value of argument(s), the additional operations are required such as the domain reduction or using different series/tables.

Code	Operation	N	L
ADD	$i+j$	1	1
SUB	$i-j$	1	1
FABS	$abs(x)$	1	1
FCHS	$-x$	1	1
FADD	$x+y$	1	3
FSUB	$x-y$	1	3
FTST	$if(x)then$	1	3
FILD	$dble(i)$	1	5
FMUL	$x*y$	1	5
FDIV	x/y	1	14–16
FSQRT	$sqrt(x)$	1	14–21
FRNDINT	$int(x)$	17	21
FYL2X	$\log_2(x)$	40–100	103
FPATAN	$atan(x)$	30–160	100–160

Here, f_{IJK} denotes the abbreviation of the function values expressed as

$$f_{IJK} \equiv f\left(X_I, Y_J, Z_K\right), \tag{9}$$

where $I, J, K \in \{P, M\}$.

The main potential function U is explicitly given (Bessel 1813) as

$$U \equiv -\left(X^2 A + Y^2 B + Z^2 C\right)/2 + YZD + ZXE + XYF, \tag{10}$$

where A through F are transcendental functions written as

$$A \equiv \tan^{-1}\left(\frac{YZ}{XR}\right), \quad B \equiv \tan^{-1}\left(\frac{ZX}{YR}\right), \quad C \equiv \tan^{-1}\left(\frac{XY}{ZR}\right), \tag{11}$$

$$D \equiv \ln(R+X), \quad E \equiv \ln(R+Y), \quad F \equiv \ln(R+Z). \tag{12}$$

Here, (i) $\tan^{-1}(T)$ denotes the principal value of the arctangent satisfying the function value condition

$$\left|\tan^{-1}(T)\right| \le \frac{\pi}{2}, \tag{13}$$

as realized by the $atan$ function in the standard mathematical libraries of C and Fortran and (ii) R is the distance from the geometric centre of the prism defined as

$$R \equiv \sqrt{X^2 + Y^2 + Z^2}. \tag{14}$$

On the other hand, the rest potential functions, U_j and U_{jk}, are defined as the partial derivatives of U (Bessel 1813) and explicitly provided (MacMillan 1930, section 43) as

$$U_X \equiv \left(\frac{\partial U}{\partial X}\right)_{Y,\,Z} = \left(\frac{\partial U}{\partial X}\right)_{Y,\,Z,\,A,\,B,\,C,\,D,\,E,\,F} = -XA + ZE + YF, \tag{15}$$

$$U_Y \equiv \left(\frac{\partial U}{\partial Y}\right)_{X,\,Z} = \left(\frac{\partial U}{\partial Y}\right)_{X,\,Z,\,A,\,B,\,C,\,D,\,E,\,F} = -YB + XF + ZD, \tag{16}$$

$$U_Z \equiv \left(\frac{\partial U}{\partial Z}\right)_{X,\,Y} = \left(\frac{\partial U}{\partial Z}\right)_{X,\,Y,\,A,\,B,\,C,\,D,\,E,\,F} = -ZC + YD + XE, \tag{17}$$

$$U_{XX} \equiv \left(\frac{\partial^2 U}{\partial X^2}\right)_{Y,\,Z} = \left(\frac{\partial U_X}{\partial X}\right)_{Y,\,Z,\,A,\,B,\,C,\,D,\,E,\,F} = -A, \tag{18}$$

$$U_{YY} \equiv \left(\frac{\partial^2 U}{\partial Y^2}\right)_{X,\,Z} = \left(\frac{\partial U_Y}{\partial Y}\right)_{X,\,Z,\,A,\,B,\,C,\,D,\,E,\,F} = -B, \tag{19}$$

$$U_{ZZ} \equiv \left(\frac{\partial^2 U}{\partial Z^2}\right)_{X,\,Y} = \left(\frac{\partial U_Z}{\partial Z}\right)_{X,\,Y,\,A,\,B,\,C,\,D,\,E,\,F} = -C, \tag{20}$$

$$U_{YZ} = U_{ZY} \equiv \left(\frac{\partial^2 U}{\partial Z \partial Y}\right)_{X} = \left(\frac{\partial U_Z}{\partial Y}\right)_{X,\,Z,\,A,\,B,\,C,\,D,\,E,\,F} = D, \tag{21}$$

$$U_{ZX} = U_{XZ} \equiv \left(\frac{\partial^2 U}{\partial X \partial Z}\right)_{Y} = \left(\frac{\partial U_X}{\partial Z}\right)_{X,\,Y,\,A,\,B,\,C,\,D,\,E,\,F} = E, \tag{22}$$

$$U_{XY} = U_{YX} \equiv \left(\frac{\partial^2 U}{\partial Y \partial X}\right)_{Z} = \left(\frac{\partial U_Y}{\partial X}\right)_{Y,\,Z,\,A,\,B,\,C,\,D,\,E,\,F} = F. \tag{23}$$

The simplification of the expression of the partial derivatives in eqs (15) through (17) is a classic trick (MacMillan 1930, section 44) as follows:

> "... As a matter of fact, however, it is not necessary to differentiate with respect to the coordinates in so far as these coordinates appear under the log and $\tan^{-1}$ symbols. It is sufficient to differentiate as though these functions were constants, and a recognition of this fact makes the differentiation a very simple matter. In order to prove this it will be observed that ..."

Although MacMillan proved the correctness of this simplification only for the gravity vector, namely in deriving the first order partial derivatives, we analytically confirmed that the same device does work for the gravity gradient tensor, namely for the second order partial derivatives (Fukushima 2018).

Note that the computation of D, E or F in the above defining forms suffer from the catastrophic precision loss when a relative coordinate, X, Y or Z, is negative, and therefore the argument of the logarithm is possibly small. A recipe to avoid this phenomenon is the introduction of a conditional switch of the argument expressions of the logarithm such as

$$D = \begin{cases} \ln(R + X), & (X \geq 0), \\ \ln\left[\left(Y^2 + Z^2\right)/(R - X)\right], & (X < 0). \end{cases} \tag{24}$$

At any rate, the number of transcendental function calls in these triple difference forms is (i) 48 for V, (ii) 24 for any of g_j and (iii) 8 for any of Γ_{jk}.

Of course, depending on the components to be evaluated simultaneously, some of the differences can be shared such that the total number of transcendental function calls is not a simple sum of the numbers for each component but significantly reduced. In fact, it becomes 48 for (iv) all of g_j, (v) all of Γ_{jk}, (vi) V and all of g_j and (vii) V and all of g_j and Γ_{jk}. Yet, these computational labors are still large so that the evaluation of the prismatic gravitational field by Bessel's method (Nagy *et al.* 2000) is time-consuming.

2.2 Fast evaluation

By utilizing the addition theorems of the logarithm and the arctangent function, eqs (1) through (3), let us rewrite the formulae given in the previous subsection.

2.2.1 Potential evaluation

First, V is rewritten as

$$\begin{aligned} V = G\rho \big[&- \left\{ \left(X_P^2 \Delta_{YZ} A_P - X_M^2 \Delta_{YZ} A_M\right) + \left(Y_P^2 \Delta_{ZX} B_P - Y_M^2 \Delta_{ZX} B_M\right) + \left(Z_P^2 \Delta_{XY} C_P - Z_M^2 \Delta_{XY} C_M\right) \right\} /2 \\ &+ \left(Y_P Z_P \Delta_X D_{PP} - Y_P Z_M \Delta_X D_{PM} - Y_M Z_P \Delta_X D_{MP} + Y_M Z_M \Delta_X D_{MM}\right) \\ &+ \left(Z_P X_P \Delta_Y E_{PP} - Z_P X_M \Delta_Y E_{PM} - Z_M X_P \Delta_Y E_{MP} + Z_M X_M \Delta_Y E_{MM}\right) \\ &+ \left(X_P Y_P \Delta_Z F_{PP} - X_P Y_M \Delta_Z F_{PM} - X_M Y_P \Delta_Z F_{MP} + X_M Y_M \Delta_Z F_{MM}\right) \big], \end{aligned} \tag{25}$$

where (i) the double differences of A, B and C, namely $\Delta_{YZ}A_J$, $\Delta_{ZX}B_J$ and $\Delta_{XY}C_J$ for $J \in \{P, M\}$, are written as

$$\Delta_{YZ} A_J \equiv \tan^{-1}\left(\frac{S_{2AJ}}{T_{2AJ}}\right) + I_{2AJ}\pi, \tag{26}$$

$$\Delta_{ZX} B_J \equiv \tan^{-1}\left(\frac{S_{2BJ}}{T_{2BJ}}\right) + I_{2BJ}\pi, \tag{27}$$

$$\Delta_{XY} C_J \equiv \tan^{-1}\left(\frac{S_{2CJ}}{T_{2CJ}}\right) + I_{2CJ}\pi, \tag{28}$$

and (ii) the single differences of D, E and F, that is $\Delta_X D_{JK}$, $\Delta_Y E_{JK}$, and $\Delta_Z F_{JK}$ for $J, K \in \{P, M\}$, are expressed as

$$\Delta_X D_{JK} \equiv \ln\left(\frac{P_{XJK}}{Q_{XJK}}\right), \quad \Delta_Y E_{JK} \equiv \ln\left(\frac{P_{YJK}}{Q_{YJK}}\right), \quad \Delta_Z F_{JK} \equiv \ln\left(\frac{P_{ZJK}}{Q_{ZJK}}\right). \tag{29}$$

Here (iii) S_{2NJ}, T_{2NJ} and I_{2NJ} are auxiliary variables computed for $N \in \{A, B, C\}$ and $J \in \{P, M\}$ as

$$S_{2NJ} \equiv S_{1NJP} T_{1NJM} - T_{1NJP} S_{1NJM}, \tag{30}$$

$$T_{2NJ} \equiv S_{1NJP} S_{1NJM} + T_{1NJP} T_{1NJM}, \tag{31}$$

$$I_{2NJ} \equiv I_{1NJP} - I_{1NJM} + \mathrm{isign2}\left(T_{1NJP} T_{1NJM} T_{2NJ}, S_{1NJP} T_{1NJP}\right), \tag{32}$$

and (iv) P_{LJK} and Q_{LJK} are another auxiliary variables conditionally calculated for $L \in \{X, Y, Z\}$ and $J, K \in \{P, M\}$ as

$$(P_{XJK}, Q_{XJK}) \equiv \begin{cases} (R_{PJK} + X_P, R_{MJK} + X_M), & (X_P \ge 0), \\ \left(Y_J^2 + Z_K^2, (R_{PJK} - X_P)(R_{MJK} + X_M)\right), & (X_P < 0 < X_M), \\ (R_{MJK} - X_M, R_{PJK} - X_P), & (X_M \le 0), \end{cases} \tag{33}$$

$$(P_{YJK}, Q_{YJK}) \equiv \begin{cases} (R_{KPJ} + Y_P, R_{KMJ} + Y_M), & (Y_P \ge 0), \\ \left(Z_J^2 + X_K^2, (R_{KPJ} - Y_P)(R_{KMJ} + Y_M)\right), & (Y_P < 0 < Y_M), \\ (R_{KMJ} - Y_M, R_{KPJ} - Y_P), & (Y_M \le 0), \end{cases} \tag{34}$$

$$(P_{ZJK}, Q_{ZJK}) \equiv \begin{cases} (R_{JKP} + Z_P, R_{JKM} + Z_M), & (Z_P \ge 0), \\ \left(X_J^2 + Y_K^2, (R_{JKP} - Z_P)(R_{JKM} + Z_M)\right), & (Z_P < 0 < Z_M), \\ (R_{JKM} - Z_M, R_{JKP} - Z_P), & (Z_M \le 0), \end{cases} \tag{35}$$

where (v) R_{IJK} is yet another auxiliary variables defined for $I, J, K \in \{P, M\}$ as

$$R_{IJK} \equiv \sqrt{X_I^2 + Y_J^2 + Z_K^2}. \tag{36}$$

In the above, (vi) S_{1NJK}, T_{1NJK} and I_{1NJK} are additional auxiliary variables written for $N \in \{A, B, C\}$ and $J, K \in \{P, M\}$ as

$$S_{1NJK} \equiv S_{NJKP} T_{NJKM} - T_{NJKP} S_{NJKM}, \tag{37}$$

$$T_{1NJK} \equiv S_{NJKP} S_{NJKM} + T_{NJKP} T_{NJKM}, \tag{38}$$

$$I_{1NJK} \equiv \mathrm{isign2}\left(T_{NJKP} T_{NJKM} T_{1NJK}, S_{NJKP} T_{NJKP}\right), \tag{39}$$

(vii) S_{NIJK} and T_{NIJK} are another additional variables prepared for $N \in \{A, B, C\}$ and $I, J, K \in \{P, M\}$ as

$$S_{AIJK} \equiv Y_J Z_K, \quad S_{BIJK} \equiv Z_J X_K, \quad S_{CIJK} \equiv X_J Y_K, \tag{40}$$

$$T_{AIJK} \equiv X_I R_{IJK}, \quad T_{BIJK} \equiv Y_I R_{KIJ}, \quad T_{CIJK} \equiv Z_I R_{JKI}, \tag{41}$$

and (viii) isign2(X, Y) is a special integer sign function defined as

$$\mathrm{isign2}(X, Y) \equiv \begin{cases} 0, & (XY \ge 0), \\ +1, & (XY < 0,\ X > 0), \\ -1, & (XY < 0,\ X < 0). \end{cases} \tag{42}$$

2.2.2 *Gravity vector evaluation*

Next, we express g_j as

$$g_X = G\rho\left[-(X_P \Delta_{YZ} A_P - X_M \Delta_{YZ} A_M) + (Z_P \Delta_{XY} E_P - Z_M \Delta_{XY} E_M) + (Y_P \Delta_{ZX} F_P - Y_M \Delta_{ZX} F_M)\right], \tag{43}$$

$$g_Y = G\rho\left[-(Y_P \Delta_{ZX} B_P - Y_M \Delta_{ZX} B_M) + (X_P \Delta_{YZ} F_P - X_M \Delta_{YZ} F_M) + (Z_P \Delta_{XY} D_P - Z_M \Delta_{XY} D_M)\right], \tag{44}$$

$$g_Z = G\rho\left[-(Z_P \Delta_{XY} C_P - Z_M \Delta_{XY} C_M) + (Y_P \Delta_{ZX} D_P - Y_M \Delta_{ZX} D_M) + (X_P \Delta_{YZ} E_P - X_M \Delta_{YZ} E_M)\right], \tag{45}$$

where (i) the double differences of A, B and C are already defined in the above and (ii) the double differences of D, E and F, namely $\Delta_{XY} D_J$, $\Delta_{ZX} D_J$, $\Delta_{YZ} E_J$, $\Delta_{XY} E_J$, $\Delta_{ZX} F_J$ and $\Delta_{YZ} F_J$ are computed as the differences of the single differences if they are available, such as in the case of the simultaneous evaluation of V, all of g_j, and all of Γ_{jk}, as

$$\Delta_{XY} D_J = \Delta_X D_{PJ} - \Delta_X D_{MJ}, \quad \Delta_{ZX} D_J = \Delta_X D_{JP} - \Delta_X D_{JM}, \tag{46}$$

$$\Delta_{YZ} E_J = \Delta_Y E_{PJ} - \Delta_Y E_{MJ}, \quad \Delta_{XY} E_J = \Delta_Y E_{JP} - \Delta_Y E_{JM}, \tag{47}$$

$$\Delta_{ZX} F_J = \Delta_Z F_{PJ} - \Delta_Z F_{MJ}, \quad \Delta_{YZ} F_J = \Delta_Z F_{JP} - \Delta_Z F_{JM}, \tag{48}$$

or (iii) the double differences of D, E and F are computed directly if the single differences are not available as

$$\Delta_{XY} D_J = \ln\left(\frac{P_{XPJ} Q_{XMJ}}{P_{XMJ} Q_{XPJ}}\right), \quad \Delta_{ZX} D_J = \ln\left(\frac{P_{XJP} Q_{XJM}}{P_{XJM} Q_{XJP}}\right), \tag{49}$$

$$\Delta_{YZ} E_J = \ln\left(\frac{P_{YPJ} Q_{YMJ}}{P_{YMJ} Q_{YPJ}}\right), \quad \Delta_{XY} E_J = \ln\left(\frac{P_{YJP} Q_{YJM}}{P_{YJM} Q_{YJP}}\right), \tag{50}$$

$$\Delta_{ZX} F_J = \ln\left(\frac{P_{ZPJ} Q_{ZMJ}}{P_{ZMJ} Q_{ZPJ}}\right), \quad \Delta_{YZ} F_J = \ln\left(\frac{P_{ZJP} Q_{ZJM}}{P_{ZJM} Q_{ZJP}}\right). \tag{51}$$

2.2.3 Gravity gradient tensor evaluation

Finally, we note that those of Γ_{jk} remain the same as

$$\Gamma_{XX} = -G\rho\Delta_3 A, \quad \Gamma_{YY} = -G\rho\Delta_3 B, \quad \Gamma_{ZZ} = -G\rho\Delta_3 C, \tag{52}$$

$$\Gamma_{YZ} = \Gamma_{ZY} = G\rho\Delta_3 D, \quad \Gamma_{ZX} = \Gamma_{XZ} = G\rho\Delta_3 E, \quad \Gamma_{XY} = \Gamma_{YX} = G\rho\Delta_3 F. \tag{53}$$

This time, (i) the triple differences of A, B and C, namely $\Delta_3 A$, $\Delta_3 B$ and $\Delta_3 C$, are computed from their double differences if they are already evaluated such as in the case of the simultaneous computation of V, all of g_j, and all of Γ_{jk} as

$$\Delta_3 A = \Delta_{YZ} A_P - \Delta_{YZ} A_M, \tag{54}$$

$$\Delta_3 B = \Delta_{ZX} B_P - \Delta_{ZX} B_M, \tag{55}$$

$$\Delta_3 C = \Delta_{XY} C_P - \Delta_{XY} C_M, \tag{56}$$

else (ii) the triple differences of A, B and C are computed directly as

$$\Delta_3 A = \tan^{-1}\left(\frac{S_{3A}}{T_{3A}}\right) + I_{3A}\pi, \tag{57}$$

$$\Delta_3 B = \tan^{-1}\left(\frac{S_{3B}}{T_{3B}}\right) + I_{3B}\pi, \tag{58}$$

$$\Delta_3 C = \tan^{-1}\left(\frac{S_{3C}}{T_{3C}}\right) + I_{3C}\pi, \tag{59}$$

where (iii) S_{3N}, T_{3N} and I_{3N} for $N \in \{A, B, C\}$ are constructed from S_{2NJ}, T_{2NJ} and I_{2NJ} for $N \in \{A, B, C\}$ and $J \in \{P, M\}$ as

$$S_{3N} \equiv S_{2NP} T_{2NM} - T_{2NP} S_{2NM}, \tag{60}$$

$$T_{3N} \equiv S_{2NP} S_{2NM} + T_{2NP} T_{2NM}, \tag{61}$$

$$I_{3N} \equiv I_{2NP} - I_{2NM} + \mathrm{isign2}\left(T_{2NP} T_{2NM} T_{3N}, S_{2NP} T_{2NP}\right). \tag{62}$$

Also, (iv) the triple differences of D, E and F, namely $\Delta_3 D$, $\Delta_3 E$ and $\Delta_3 F$, are computed from their double differences if they are already available such as in the case of the simultaneous calculation of V, all of g_j, and all of Γ_{jk} as

$$\Delta_3 D = \Delta_{XY} D_P - \Delta_{XY} D_M, \tag{63}$$

$$\Delta_3 E = \Delta_{YZ} E_P - \Delta_{YZ} E_M, \tag{64}$$

$$\Delta_3 F = \Delta_{ZX} F_P - \Delta_{ZX} F_M, \tag{65}$$

(v) the triple differences of D, E and F are computed from their single differences if they are already computed but their double differences are not such as in the case of the simultaneous preparation of V and all of Γ_{jk} as

$$\Delta_3 D = \Delta_X D_{PP} - \Delta_X D_{PM} - \Delta_X D_{MP} + \Delta_X D_{MM}, \tag{66}$$

$$\Delta_3 E = \Delta_Y E_{PP} - \Delta_Y E_{PM} - \Delta_Y E_{MP} + \Delta_Y E_{MM}, \tag{67}$$

$$\Delta_3 F = \Delta_Z F_{PP} - \Delta_Z F_{PM} - \Delta_Z F_{MP} + \Delta_Z F_{MM}, \tag{68}$$

or (vi) the triple differences of D, E and F are computed directly if neither the single nor the double differences are available:

$$\Delta_3 D = \ln\left(\frac{P_{XPP} P_{XMM} Q_{XPM} Q_{XMP}}{P_{XPM} P_{XMP} Q_{XPP} Q_{XMM}}\right), \tag{69}$$

$$\Delta_3 E = \ln\left(\frac{P_{YPP}P_{YMM}Q_{YPM}Q_{YMP}}{P_{YPM}P_{YMP}Q_{YPP}Q_{YMM}}\right), \tag{70}$$

$$\Delta_3 F = \ln\left(\frac{P_{ZPP}P_{ZMM}Q_{ZPM}Q_{ZMP}}{P_{ZPM}P_{ZMP}Q_{ZPP}Q_{ZMM}}\right). \tag{71}$$

2.2.4 Computational notes

In the above formulae, there exist computational difficulties of (i) zero division in evaluating the arguments of the arctangent function and the logarithm and (ii) zero argument of the logarithm. These problems can be resolved (i) by replacing $\tan^{-1}(S/T)$ with a two argument function $arctan2(S, T)$ defined as

$$arctan2(S, T) = \begin{cases} atan(S/T), & (T \neq 0), \\ \pi/2, & (T = 0; S > 0), \\ -\pi/2, & (T = 0; S < 0), \\ 0, & (T = 0; S = 0), \end{cases} \tag{72}$$

and (ii) by adding a tiny positive quantity to both the numerator and the denominator of the fractional form of the logarithm argument such as $\ln[(P_{LJK} + \eta)/(Q_{LJK} + \eta)]$ instead of $\ln(P_{LJK}/Q_{LJK})$ where η is a constant defined as $\eta \equiv 10^{-150}$.

In the above, the two procedures, namely (i) the replacement of the tangent argument S/T by the argument pair (S; T) and (ii) the introduction of the intermediate variables P_{LJK} and Q_{LJK}, have both been introduced so as to reduce the total number of the divisions, which are relatively time-consuming when compared with those of the multiplication and the addition/subtraction as clearly indicated in Table 3. Also, the functions I_{1NJK}, I_{2NJ} and I_{3N} provide a mechanism for the separate accumulation of the integer multiples of π. This allows unnecessary multiplications of real numbers to be avoided, and avoids the increase of the round-off errors caused by the addition of multiples of π to the angles.

2.2.5 Remarks

The physical meaning of these rewriting is as follows: (i) the first six terms in eq. (25) are the sum of the signed arctangent terms evaluated on certain faces of prism, (ii) the rest 12 terms in eq. (25) are the sums of logarithms of the signed terms evaluated on certain edges of the prism, (iii) the first pair of the terms in eqs (43) through (45) denotes the similar arctangent component on the faces of the prism, and (iv) the rest four terms in eqs (43) through (45) are the similar sum of logarithms on the edges of the prism.

In any case, these rewritten expressions are useful for the fast computation of V, g_j and/or Γ_{jk}. In fact, the number of transcendental functions called in the new method is significantly less than that in Bessel's method (Nagy *et al.* 2000) as (i) 18 for V, (ii) 6 for any of g_j, (iii) 1 for any of Γ_{jk}, (iv) 18 for all of g_j, (v) 6 for all of Γ_{jk}, (vi) 18 for V and all of g_j and (vii) 18 for V and all of g_j and Γ_{jk}, as already listed in Table 2. Therefore, the new method is expected to run 2.7–8.0 times faster than Bessel's method, provided various computational overheads are ignored, for the square root, the four arithmetic operations, conditional judgements and other non-transcendental operations.

None the less, it is also true that this reduction is achieved at the cost of additional computational operations described in the above. Since (i) the increase of the computational labor associated with these additional operations is not negligible as shown in Table 2 and (ii) the acceleration factor estimated in the above does depend on the optimization the execution code compilation, we must measure the actual speed-up factor by certain numerical experiments as will be illustrated next.

3 NUMERICAL EXPERIMENTS

3.1 Computational speed

Let us present the results of some numerical experiments on the new method developed in the previous section. We begin with the computational speed. Table 1 has already compared the averaged CPU times to evaluate various combinations of (i) the gravitational potential, V, (ii) the jth rectangular component of the gravity vector, g_j and (iii) the jkth rectangular component of the gravity gradient tensor, Γ_{jk}. The compared methods are Bessel's method (Nagy *et al.* 2000) and the new method described in the previous section.

The experiments were executed in the double precision environment for a practical case, namely the evaluation of the gravitational field quantities at the central point on the top surface of the 225 × 150 prisms consisting of the local land mass near Mt Fuji, the profiles of which are shown in the previous work of ours (Fukushima 2020). The shape of each prism is very fine as 5.0 m × 6.2 m × 1800–2300 m although the whole land mass is nearly cubic as 1152 m × 930 m × ≈2000 m. We counted the gravitational effects caused by the 225 × 150 prisms as a whole by assuming the homogeneity of the density of these prisms. Since all the evaluation points are within or without but sufficiently close to the Brillouin sphere of each of prism, only the direct computation of the exact formula provides reliable results (Fukushima 2020). In any case, the amount of the total computation is so large as $(225 \times 150)^2 \approx 1.14 \times 10^9$ executions of the prism-to-a-point evaluation.

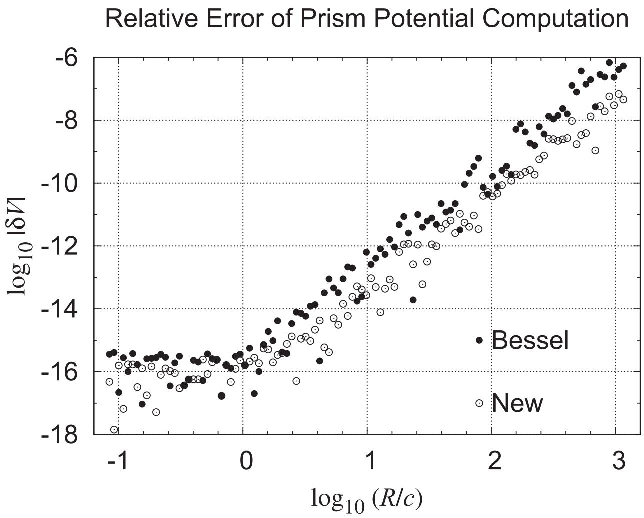

Figure 2. Relative error of prismatic gravitational potential computation. Plotted are the relative errors of Bessel's method (Nagy *et al.* 2000) and the new method to evaluate the exact analytical formula of the gravitational potential computation of a uniform prism. The relative errors are defined as $\delta V \equiv (\Delta V)/V$ where the raw errors, $\Delta V \equiv V_{\mathrm{computed}} - V_{\mathrm{reference}}$, are measured by comparing with the quadruple precision computation of Bessel's method as the reference value. The error values are plotted along a line of constant direction starting from the geometric centre of the prism in a log–log manner with respect to R/c, the normalized radius from the geometric centre of the prism. When outside the Brillouin radius of the prism, where $R/c \approx 1.28$, both of the errors increase cubically with respect to the distance from the prism geometric centre.

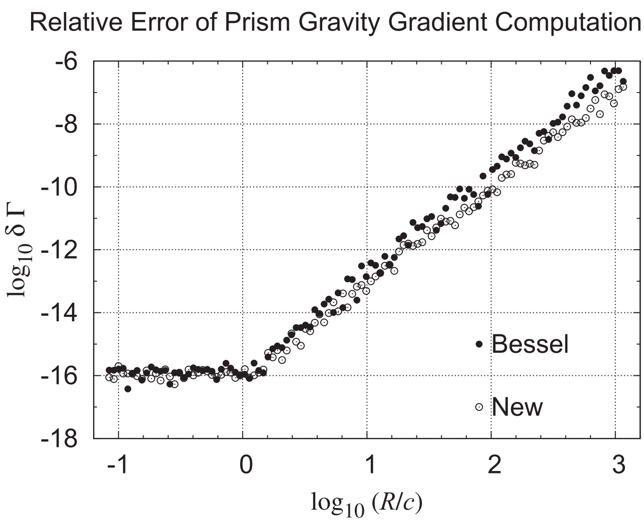

Figure 4. Relative error of gravity gradient computation of a nearly cubic prism. Same as Fig. 2 but for the relative errors of the gravity gradient tensor, $\delta\Gamma \equiv |\Delta\Gamma|/|\Gamma|$.

All the computer codes were written in Fortran 90 and compiled by the Intel Parallel Studio XE 2019 Update 4 Composer for Fortran, or the so-called `ifort 19.0`, with the maximum optimization flags. The CPU times were measured at a consumer PC with the Intel Core i7-8750H CPU running at 2.20 GHz clock. The computation was done under the Windows 10 OS in the single-core-single-thread mode. Table 1 has already illustrated that the new method is 2.3–4.2 times faster than Bessel's method depending on the combination of the field quantities to be computed simultaneously.

This acceleration is mainly caused by the reduction of the transcendental function calls already summarized in Table 2. Nevertheless, the measured acceleration factors are significantly smaller than those expected from the numbers of the transcendental function calls. This is due to the increased number of arithmetic operations required by the new method, as also illustrated in Table 2.

3.2 Computational error

We move on to the aspect of the computational error. For this purpose, we prepared Figs 2 to 4 comparing the relative errors of Bessel's method and the new method in computing the gravitational potential, the gravity vector and the gravity gradient tensor, respectively. Although the prism chosen is nearly cubic such that its normalized half-dimensions are $a = 2.5$, $b = 3.1$ and $c = 5.0$, the computational errors do not depend on these conditions, and therefore the obtained results are generic.

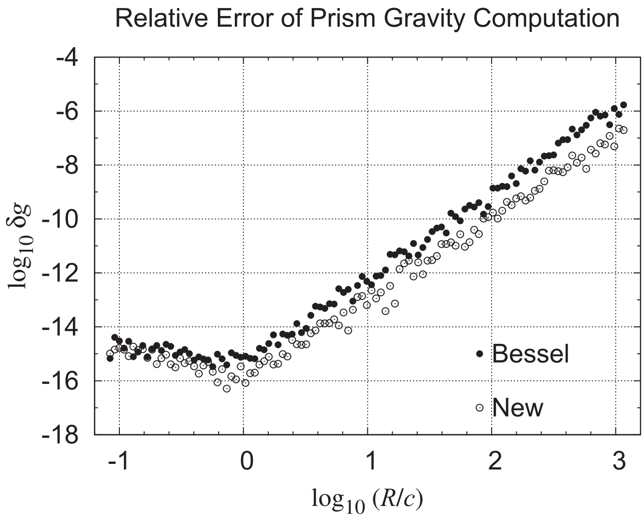

Figure 3. Relative error of gravity computation of a nearly cubic prism. Same as Fig. 2 but for the relative errors of the gravitational acceleration vector, $\delta g \equiv |\Delta \mathbf{g}|/|\mathbf{g}|$.

The errors were first measured as the direct difference from the quadruple precision computation by using Bessel's method. Then, they were normalized as

$$\delta V \equiv \frac{\Delta V}{V}, \tag{73}$$

$$\delta g \equiv \frac{|\Delta \mathbf{g}|}{|\mathbf{g}|} = \sqrt{\frac{(\Delta g_X)^2 + (\Delta g_Y)^2 + (\Delta g_Z)^2}{g_X^2 + g_Y^2 + g_Z^2}}, \tag{74}$$

$$\delta \Gamma \equiv \frac{|\Delta \Gamma|}{|\Gamma|} = \sqrt{\frac{(\Delta \Gamma_{XX})^2 + (\Delta \Gamma_{YY})^2 + (\Delta \Gamma_{ZZ})^2 + 2(\Delta \Gamma_{YZ})^2 + 2(\Delta \Gamma_{ZX})^2 + 2(\Delta \Gamma_{XY})^2}{\Gamma_{XX}^2 + \Gamma_{YY}^2 + \Gamma_{ZZ}^2 + 2\Gamma_{YZ}^2 + 2\Gamma_{ZX}^2 + 2\Gamma_{XY}^2}}, \tag{75}$$

where ΔV through $\Delta \Gamma_{ZZ}$ are the raw values of the difference from the quadruple precision computation. These errors are evaluated along a straight survey line directed away from the geometric centre of the prism with a non-trivial direction where both the latitude and the longitude are 45°. All these figures plot the relative errors as log–log graphs with respect to the distance from the geometric centre of the prism, R, for the range $0.1 \le R/c \le 10^3$. Clearly, both of the results stay at the machine epsilon level inside the Brillouin sphere and grow cubically outside it. This is a well-known phenomenon (Forsberg 1984; Holstein & Ketterridge 1996). In average, the relative errors of the new method are somewhat smaller than those of Bessel's method, say by the factor of 2–10. This is thanks to the various efforts to reduce the information loss in the new method, which would be caused by the difference of similar quantities in the basic operations.

4 CONCLUSION

In order to accelerate Bessel's method to evaluate the exact analytical formulae of the gravitational field of a uniform rectangular prism by using the triple difference of certain analytic functions (Bessel 1813; Nagy *et al.* 2000), we utilized the addition theorems of the logarithm and the arctangent function while taking care of the ambiguity factor of the arctangent function properly so as to develop a new method to evaluate the triple differences quickly. Exactly the same approach is applicable to the geomagnetic field computation.

The new method is fast mainly because the number of transcendental functions required in the evaluation procedure is significantly reduced by the factor 2.7–8.0. Actually, we confirmed the superiority of the new method by some numerical experiments such that it runs 2.3, 2.3 and 3.7 times faster than Bessel's method in computing the gravitational potential, the gravity vector and the gravity gradient tensor, respectively. Also, we find that the computational errors of the new method are smaller than those of Bessel's method, say by the factor 2–10 in general. In conclusion, the new method is faster and more precise than Bessel's method.

For the readers' convenience, we prepared *xfpri2.txt*, a plain text file containing the Fortran 90 test program package to compute various combinations of the prismatic gravitational potential, gravity vector and gravity gradient tensor by the new method and their test outputs. It is freely available at the author's web site:

https://www.researchgate.net/profile/Toshio_Fukushima

ACKNOWLEDGEMENTS

The author appreciates valuable suggestions and fruitful comments by Prof H. Holstein and anonymous referee to improve the quality and readability of the article.

REFERENCES

Amante, C., 2009. Etopo1: 1 arc-minute global relief model: procedures, data sources and analysis, http://www.ngdc.noaa.gov/mgg/global/global.html.

Banerjee, B. & Das Gupta, S.P., 1977. Gravitational attraction of a rectangular parallelepiped, *Geophys.,* **42,** 1053–1055.

Benedek, J., Papp, G. & Kalmár, J., 2018. Generalization techniques to reduce the number of volume elements for terrain effect calculations in fully analytical gravitational modelling, *J. Geod.,* **92,** 361–381.

Bessel, F.W., 1813. Auszug aus einem Schreiben des Herrn Prof. Bessel, *Monatl. Corresp. Bef. Erd- und Himmels-Kunde,* **XXVII,** 80–85.

Blakeley, R.J., 1996. *Potential Theory in Gravity and Magnetic Applications,* Cambridge Univ. Press.

Bronshtein, I.N., Semendyayev, K.A., Musiol, G. & Mühlig, H., 2015. *Handbook of Mathematics,* 6th edn, Springer.

de Pater, I. & Lissauer, J.J., 2010. *Planetary Sciences,* 2nd edn, Cambridge Univ. Press.

Faires, J.D. & Faires, B.D., 1989. *Calculus of One Variable,* 2nd edn, Random House Inc.

Featherstone, W.E. & Kirby, J.F., 2002. New high-resolution grid of gravimetric terrain corrections over Australia, *Austr. J. Earth Sci.,* **49,** 733–734.

Forsberg, R., 1984. A study of terrain reductions, density anomalies and geophysical inversion methods in gravity field modelling, Report 355, Department of Geodetic Science and Surveying, Ohio State University, Columbus.

Forsberg, R. & Tscherning, C.C., 1981. The use of height data in gravity field approximation by collocation, *J. geophys. Res.,* **86,** 7843–7854.

Fukushima, T., 2018. Recursive computation of gravitational field of a right rectangular parallelepiped with density varying vertically by following an arbitrary degree polynomial, *Geophys. J. Int.,* **215,** 864–879.

Fukushima, T., 2020. Taylor series expansion of prismatic gravitational field, *Geophys. J. Int.,* **220,** 610–660.

Garcia-Abdeslem, J., 1992. Gravitational attraction of a rectangular prism with depth-dependent density, *Geophys.,* **57,** 470–473.

Garcia-Abdeslem, J., 2005. Gravitational attraction of a rectangular prism with density varying with depth following a cubic polynomial, *Geophys.,* **70,** J39–J42.

Geospatial Information Authority of Japan. 2012. *National Land Numerical Information,* http://nlftp.mlit.go.jp/ksj-e/index.html.

Heck, B. & Seitz, K., 2007. A comparison of the tesseroid, prism and point-mass approaches for mass reductions in gravity field modelling, *J. Geod.,* **81,** 121–136.

Heiskanen, W.A. & Moritz, H., 1967. *Physical Geodesy,* Freeman.

Henry, E.C. & Penny, D.E., 2002. *Calculus,* 6th edn, Prentice Hall.

Hirt, C., 2018. Artefact detection in global digital elevation models (DEMs): the maximum slope approach and its application for complete screening of the SRTM v4.1 and MERIT DEMs, *Remote Sens. Environ.,* **207,** 27–41.

Hirt, C., Reusner, E., Rexer, M. & Kuhn, M., 2016. Topographic gravity modelling for global Bouguer maps to degree 2,160: validation of spectral and spatial domain forward modelling techniques at the 10 microgal level, *J. geophys. Res.,* **121,** 6846–6862.

Hirt, C., Yang, M., Kuhn, M., Bucha, B., Kurzmann, A. & Pail, R., 2019. SRTM2gravity: an ultra-high resolution global model of gravimetric terrain corrections, *Geophys. Res. Lett.,* **46** (9), 4618–4627.

Holstein, H. & Ketterridge, B., 1996. Gravimagnetic analysis of uniform polyhedral, *Geophysics,* **61,** 357–364.

Holstein, H., Schurholz, P., Starr, A.J. & Chakraborty, M., 1999. Comparison of gravimetric formulas for uniform polyhedra, *Geophysics,* **64,** 1438–1446.

Ivan, M., 1990. Comment on "Optimum expression for computation of the gravity expression for computation of the gravity field of a homogeneous polyhedral body" by V. Pohanka., *Geophys. Prospect.,* **38,** 331–332.

Jekeli, C., 2007. Potential theory and static gravity field of the earth, in *Treatise on Geophysics,* 2nd edn, Vol. **3,** Chap. 3.02, ed. Schubert, G., Elsevier B.V.

Jiang, L., Zhang, J.-Z. & Feng, Z.-B., 2017. A versatile solution for the gravity anomaly of 3D prism-meshed bodies with depth-dependent density contrast, *Geophysics,* **82,** G77–G86.

Jiang, L., Liu, J., Zhang, J.-Z. & Feng, Z.-B., 2018. Analytic expressions for the gravity gradient tensor of 3D prisms with depth-dependent density, *Surv. Geophys.,* **39,** 337–368.

Kalmár, J., Papp, G. & Szabó, T., 1995. DTM-based surface and volume approximation: geophysical application, *Comp. Geosci.,* **21,** 245–257.

Kellogg, O.D., 1929. *Foundations of Potential Theory,* Springer.

MacMillan, W.D., 1930. *The Theory of the Potential,* McGraw-Hill.

Mader, K., 1951. Das Newtonsche Raumpotential prismatischer Korper und seine Ableitungen bis zur dritten Ordnung, *Osterr. Z. Vermess. Sonderheft 11 der Osterreichischen Zeitschrift für Vermessungswesen,* **11.**

Mollweide, K.B., 1813. Auflösung einiger die Anziehung von Linien Flächen und Körpern betreffenden Aufgaben unter denen auch die in der Monatl. Corresp. Bd XXIV. S. 522. vorgelegte sich findet, *Monatl. Corresp. Bef. Erd- und Himmels-Kunde,* **XXVII,** 26–38.

Moritz, H., 1980. *Advanced Physical Geodesy,* Herbert Wichmann.

Nagy, D., 1966. The gravitational attraction of a right rectangular prism, *Geophys.,* **31,** 362–371.

Nagy, D., 1988. A short program for three-dimensional gravity modeling, *Acta Geod. Geoph. Mont. Hung.,* **23,** 449–459.

Nagy, D., Papp, G. & Benedek, J., 2000. The gravitational potential and its derivatives for the prism, *J. Geod.,* **74,** 552–560.

Olver, F.W.J., Lozier, D.W., Boisvert, R.F. & Clark, C.W.(eds), 2010. *NIST Handbook of Mathematical Functions,* Cambridge Univ. Press.

Pohanka, V., 1988. Optimum expression for computation of the gravity field of a homogeneous polyhedral body, *Geophys. Prospect.,* **36,** 733–751.

Pohanka, V., 1990. Reply to comment by M. Ivan, *Geophys. Prospect.,* **38,** 333–335.

Pohanka, V., 1998. Optimum expression for computation of the gravity field of a polyhedral body with linearly increasing density, *Geophys. Prospect.,* **46,** 391–404.

Rao, D.B. & Babu, N.R., 1991. A Fortran-77 computer program for three-dimensional analysis of gravity anomalies with variable density contrast, *Comp. Geosci.,* **17,** 655–667.

Rao, D.B. & Babu, N.R., 1993. A Fortran-77 computer program for three-dimensional inversion of magnetic anomalies resulting from multiple prismatic bodies, *Comp. Geosci.,* **19,** 781–801.

Ren, Z.-Y., Chen, C.-J., Pan, K., Kalscheuer, T., Maurer, H. & Tang, J.-T., 2017. Gravity anomalies of arbitrary 3D polyhedral bodies with horizontal and vertical mass contrasts, *Surv. Geophys.,* **38,** 479–502.

Rodriguez, E., Morris, C.S. & Belz, J.E., 2006. A global assessment of the SRTM performance, *Photogr. Eng. Remote Sens.,* **72,** 249–260.

Smith, B. & Sandwell, D., 2003. Accuracy and resolution of shuttle radar topography mission data, *Geophys. Res. Lett.,* **32,** L21S01.

Stacey, F.D. & Davis, P.M., 2008. *Physics of the Earth,* 4th edn, Cambridge Univ. Press.

Stewart, J., 2014. *Single Variable Calculus: Early Transcendentals,* 8th edn, Cengage Learning.

Strakhov, V.N., Lapina, M.I. & A B Yefimov, A.B., 1986. A solution to forward problems in gravity and magnetism with new analytical expressions for the field elements of standard approximating bodies I, *Izv., Earth Sci.,* **22,** 471–482.

Strakhov, V.N. & Lapina, M.I., 1986. Solution of direct gravity and magnetic problems with new analytical expressions of the field of typical approximating bodies II, *Izv., Earth Sci.,* **22,** 566–575.

Tachikawa, T., Hato, M., Kaku, M. & Iwasaki, A., 2011. Characteristics of ASTER GDEM version 2, *Proc. IEEE Int. Geosci. Remote Sensing Symp.,* **2011,** 3657–3660.

Tsoulis, D., 2001. Terrain correction computations for a densely sampled DTM in the Bavarian Alps, *J. Geod.,* **75,** 291–307.

Vog, A., 2019. Instruction Tables (2019-08-15), https://www.agner.org/optimize/instruction_tables.pdf.

Wild-Pfeiffer, F., 2008. A comparison of different mass elements for use in gravity gradiometry, *J. Geod.,* **82,** 637–653.

Yamazaki, D. *et al.*, 2017. A high accuracy map of global terrain elevations, *Geophys. Res. Lett.,* **44,** 5844–5853.

Zhang, J.-Z. & Jiang, L., 2017. Analytical expressions for the gravitational vector field of a 3-D rectangular prism with density varying as an arbitrary-order polynomial function, *Geophys. J. Int.,* **210,** 1176–1190.